

EXPERIMENTAL CHARACTERIZATION OF ALUMINUM FIBRE/SAPO-34 COMPOSITES FOR ADSORPTION HEAT PUMP APPLICATIONS

Andreas Velte^{1*}, Ralph Herrmann², Olaf Andersen³, Ursula Wittstadt¹,
Gerrit Földner¹, Lena Schnabel¹

¹Fraunhofer Institute for Solar Energy Systems (ISE), Division Thermal Systems and Buildings, Heidenhofstraße 2,
79110 Freiburg, Germany
andreas.velte@ise.fraunhofer.de

²SorTech AG, Zscherbener Landstraße 17, 06126 Halle (Saale), Germany
ralph.herrmann@sortech.de

³Fraunhofer Institute for Manufacturing and Advanced Materials IFAM, Branch Lab Dresden, Winterbergstraße 28, 01277
Dresden, Germany
olaf.andersen@ifam-dd.fraunhofer.de

NOMENCLATURE LIST

Symbol	Description	Unit	Symbol	Description	Unit
d_{cmp}	Thickness of the metal adsorbent composite	m	T_{cldPlt}	Coldplate temperature	K
Ψ_{pre}	Porosity of uncoated fibres	-	T_{eqi}	Equilibrium temperature	K
$d_{\text{fib,pre}}$	Diameter of uncoated fibres	m	X	Loading	kg/kg
a, b	Length and width of the sample	m	P_{v}	Power density	W/dm ³
M_{sorb}	Adsorbent mass	kg	Δh_{ads}	Adsorption enthalpy	J/kg
d_{cryst}	Adsorbent layer thickness	m	M_{fib}	Mass of fibres	kg
d_{maP}	Macro pore diameter	m	t	Time	s
T_{srf}	Surface temperature of sample	K			

ABSTRACT

The development of thermally driven adsorptive heat pumps is strongly linked with the understanding of the dynamics of the adsorption process within the adsorption heat exchanger, which is the key component of adsorption systems. In recent years, much effort has been put in developing adsorption heat exchangers providing a good mass transfer in the adsorbent bed and a good heat transfer between adsorbent and metal structure of the adsorption heat exchanger (Dawoud 2013; Aristov 2014; Földner 2015).

Aluminum based fibrous structures have a high surface area in the order of magnitude $10^4 \text{ m}^2/\text{m}^3$, a good thermal conductivity of 5...30 W/(m·K) and a high porosity between 60 % and 80 % (Andersen et al. 2007), which makes them a promising metal support for adsorption heat exchanger designs. With the technique of partial support transformation (PST) it is possible to grow SAPO-34 crystals directly on the aluminum fibres, which leads to low thermal contact resistances ($10^{-5} \text{ m}^2\cdot\text{K}/\text{W}$) between adsorbent and metal (Bauer et al. 2009). The adsorption kinetics of such structures was analyzed (Wittstadt et al. 2015) and modeled (Földner 2015) with a detailed model of the heat and mass transfer processes in the fibrous structure as well as the adsorbent layer. The thermal contact between the fibrous plate and the metal support as well as the thickness of the adsorbent layer were found to be important parameters for a further improvement of the power density of these composite materials. Further degrees of freedom are the porosity, the thickness of the composite and fibre properties (length, diameter).

In order to base the theoretical geometry optimization on a solid experimental basis, a set of 26 small scale samples (max. base area of 43·43 mm²) as shown in Figure 1 was manufactured and experimentally characterized in the last two years.

Here, the measurement results of the most promising samples are presented. The evaluation includes the calculation of driving temperature differences, which makes it possible to differentiate between heat and mass transfer resistances without fitting the experimental data with numerical models. Finally, a possible path for further improvements of the power density of these composite materials is shown.

SAMPLE PREPARATION AND PROPERTIES

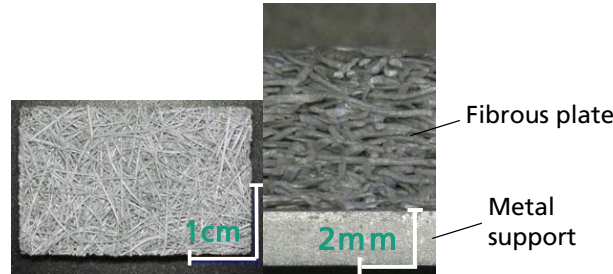


Figure 1 – Aluminum fibre/SAPO-34 composite sample, top view (left), side view (right)

An overview of the most important sample properties is listed in Table 1. Following quantities in Table 1 were measured directly:

- the thickness of the fibrous plate d_{cmp} is approximately 3 mm or 5 mm,
- the porosity of the uncoated fibrous structures is between ψ_{pre} 70 % and 80 %
- the length of the uncoated fibres is 6 mm or 12 mm, the diameter $d_{\text{fib,pre}}$ is 110 μm , 123 μm or 185 μm
- Length a and length b of the sample

The adsorbent mass M_{sorb} was measured after the PST process with two different methods. Following quantities were calculated using geometric correlations and the model of a cylindrical pore:

- the mean thickness of the adsorbent layer on the fibres d_{cryst} is between 14 μm and 27 μm
- the macro pore diameter d_{maP} is between 119 μm and 625 μm

The fibrous plate is sintered on the metal support, except for sample 8. In this case, the fibrous plate is glued on the metal support.

Table 1 – Properties of the measured samples

Sample	a in mm	b in mm	d_{cmp} in mm	$d_{\text{fib,pre}}$ in μm	M_{sorb} in g	d_{cryst} in μm	d_{maP} in μm	ψ_{pre}	$M_{\text{sorb}}/M_{\text{fib}}$
1 ¹	35.4	20.1	2.9	123	0.83	24	214	0.70	0.72
2	43.2	43.2	3.0	185	0.59	14	625	0.786	0.23
3 ¹	35.4	20.1	2.9	123	0.64	18	195	0.70	0.44
4 ²	56.3	20.1	2.8	110	0.88	23	360	0.80	0.86
5 ²	56.3	20.1	2.9	110	0.91	22	343	0.80	0.83
6 ³	22.5	20.1	5.0	110	1.18	26	151	0.71	0.89
7 ³	22.5	20.1	5.0	110	1.21	24	119	0.71	0.71
8	36.7	20.1	5.7	185	1.02	27	457	0.75	0.49

MEASUREMENTS

The experimental characterization of the adsorption dynamics is based on adsorption measurements with the method of the large pressure jump (LPJ). All measurements were performed at Fraunhofer ISE in the

¹ The superscripts 1, 2, and 3 indicate that these pairs have the same fibrous structure, but their adsorbent mass differs. Furthermore, the metal mass of the fibrous structure after the PST process is different for these pairs. Thus, they differ also in their macro pore diameter.

kinetic measurement test facility described by Frazzica, Földner et al. (Frazzica et al. 2014). The pressure and steam temperature are measured, the water uptake during a measurement is calculated using the law of the ideal gas. All samples were measured under the same conditions: the temperature of coldplate was kept constant at 40 °C throughout the measurement, temperature of desorption was 95 °C at a pressure of 42 mbar, starting pressure of the adsorption was 23 mbar. This results in an initial loading between 0.05 kg/kg and 0.06 kg for all samples and a loading difference between 0.16 kg/kg and 0.23 kg/kg.

ADSORPTION DYNAMICS

The adsorption dynamics are compared by calculating the rise up time between 15 % and 80 % relative loading. The results for all 8 samples are shown in Figure 2 (secondary y-axis on the right). By comparing sample properties and the results for the adsorption dynamics, following conclusions can be drawn:

- A strong dependence of adsorption dynamics on the **adsorbent layer thickness** d_{crist} is observed
- A significant difference between samples with 3 mm and 5 mm **thickness of composite** can be seen, e. g. the rise up time is up to twice as high as could be expected from samples with the same adsorbent layer thickness.
- Samples 4 and 5 have nearly the same dynamics as sample 1, which is not a mass transfer limitation, since the macro pores of these samples are larger than the macro pores of sample 1 and the mean adsorbent layer thickness is smaller than it is for sample 1
- The influence of **macro pore size** can be seen in comparing sample 8 with samples 6 and 7. Sample 8 has a macro pores diameter, which is up to four times larger than the macro pore diameters of sample 6 and sample 7. Thus, the rise up time of sample 8 is lower than it is for sample 6 and sample 7, although the adsorbent layer thickness of sample 8 is slightly higher than it is for all other samples.

Since the surface temperature of the samples is measured and evaluated a more differentiated comparison of the samples is possible.

EVALUATION OF DRIVING TEMPERATURE DIFFERENCES

The surface temperature of the sample T_{srf} is measured with an infrared sensor. Although the temperature differs within the sample, this value is taken as a measure for the mean adsorbent temperature. The temperature difference of heat transfer is calculated using this temperature according to equation [1].

$$\Delta T_{\text{htTm}} = T_{\text{srf}} - T_{\text{cldPlt}} \quad [1]$$

The temperature difference of mass transfer is defined in equation [2] as the difference between adsorbent equilibrium temperature $T_{\text{eqi}}(p, X)$ and the surface temperature of the sample.

$$\Delta T_{\text{massTm}} = T_{\text{eqi}}(p, X) - T_{\text{srf}} \quad [2]$$

In order to compare the time dependent temperature differences for all samples on the same basis, the temperature differences are integrated and weighted using the gradient of the loading, according to equation [3].

$$\Delta T_{\text{mean}} = \frac{\int_0^t \Delta T \cdot \frac{dX}{dt} \cdot dt}{\int_0^t \frac{dX}{dt} \cdot dt} \quad [3]$$

The weighted temperature differences of heat and mass transfer are shown in Figure 2. For the measurement conditions presented here, the overall temperature difference of all samples is approximately 16 K. Thus, all measurements were conducted having nearly the same driving temperature difference.

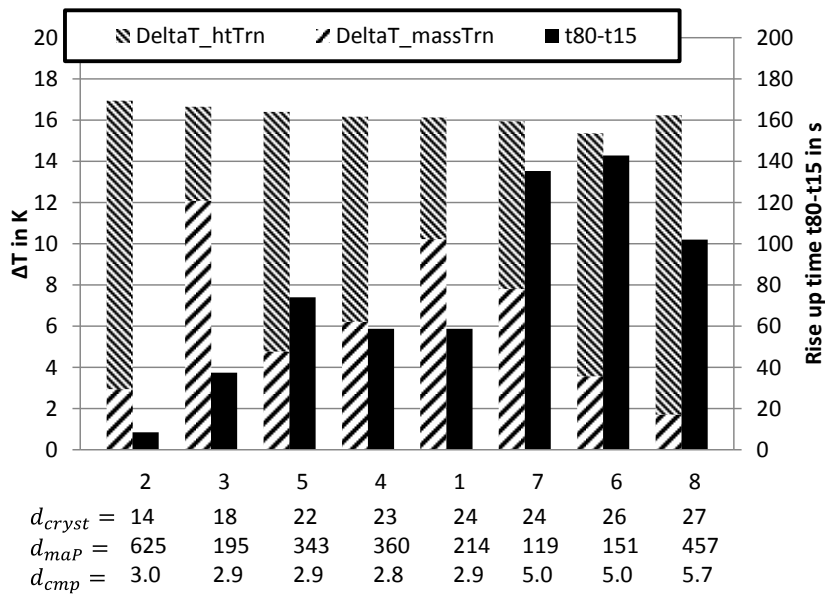


Figure 2 – Temperature differences (primary y-axis, left) and rise up times (secondary y-axis, right) of LPJ HP measurements of all samples. All measurements have nearly the same overall driving temperature difference (approx.. 16 K).

By differentiating between the temperature difference of heat and mass transfer the limiting factors can be identified for each sample:

- The **heat transfer limitation** is dominating the measurements of samples 2 and 9. Since both samples have completely different properties, this results in huge differences regarding the time constants. The **thin adsorbent layer** of sample 2 leads to **small rise up times** (fast adsorption dynamics). Thus, the sample is heating up quickly in the beginning of adsorption and the rest of the adsorption process depends on how good the heat is transferred to the coldplate. In case of sample 8 the heat transfer limitation is due to the bad thermal coupling between the fibrous plate and the metal support, which leads to a high rise up time.
- The fibres of sample 1 and sample 3 are similar, but the adsorbent coating differs in its layer thickness. Sample 3 was expected to have a lower mass transfer limitation than sample 1, which is not the case. It seems that also the coupling between fibrous plate and metal support is different for both samples, thus **both a better heat transfer and a thinner adsorbent layer** contribute to fast adsorption dynamics in case of sample 3.
- If sample 1 and sample 5 are compared, it is obvious that the slightly slower adsorption kinetics of sample 5 is due to a **higher heat transfer resistance** between fibrous plate and metal support and a **worse thermal conductivity of the fibrous structure**. The measured effective thermal conductivity² of sample 1 is much higher than it is for sample 5 (8.711 W/(m·K) and 2.812 W/(m·K)). The adsorbent layer thickness of sample 5 is thinner and the macro pore size is larger, which would rather accelerate the adsorption dynamics instead of slowing it down.
- Sample 1 and sample 6 have nearly the same adsorbent layer thickness. The difference between these samples is the **thickness of the metal adsorbent composite**, which is 3 mm in case of sample 1 and 5 mm in case of sample 6. The temperature differences of sample 6 indicate a strong heat transfer limitation, which is plausible, since the thermal resistance increases with an increasing thickness of the metal adsorbent composite. Furthermore, the measured effective thermal conductivity² of sample 1 is more than twice as high as it is for sample 6 (8.711 W/(m·K)

² The thermal conductivity measurements are performed before the samples are directly crystallized, thus these values are only an indicator for the true thermal conductivity of the samples. However, the effective thermal conductivity is a combination of the heat transfer in the composite, which depends mainly on the fibre diameter and the porosity, and the heat transfer resistance between fibrous plate and metal support.

and 4.128 W/(m·K)), which also increases the heat transfer resistance and helps to explain the strong heat transfer limitation of sample 6.

- If sample 6 and sample 8 are compared, the **mass transport limitation** of sample 6 caused by the much **smaller macro pores** of sample 6 becomes visible. The temperature difference of mass transfer of sample 6 is twice as high as it is for sample 8. Although sample 8 has a thicker adsorbent layer and a bad thermal coupling between fibrous plate and metal support (since sample 8 is glued and sample 6 is sintered), it shows faster adsorption dynamics than sample 6, which can only be explained with the smaller macro pores of sample 6.

POWER DENSITY

The mean power density of the composite is defined in equation[4]. The main factor for the power density is the adsorption dynamics, which is the ratio of absolute loading difference between 15 % and 80 % relative loading and the rise up time.

$$P_V = \frac{M_{sorb}}{a \cdot b \cdot d_{cmp}} \cdot \Delta h_{ads} \cdot \frac{X_{80} - X_{15}}{t_{80} - t_{15}} \quad [4]$$

The ratio of adsorbent mass M_{sorb} and mass of the fibres M_{fib} is an indicator for the COP, which can be achieved in a cycle without heat recovery (low ratio means low COP, high ratio means high COP). In Figure 3 the power density is plotted over this ratio for all samples.

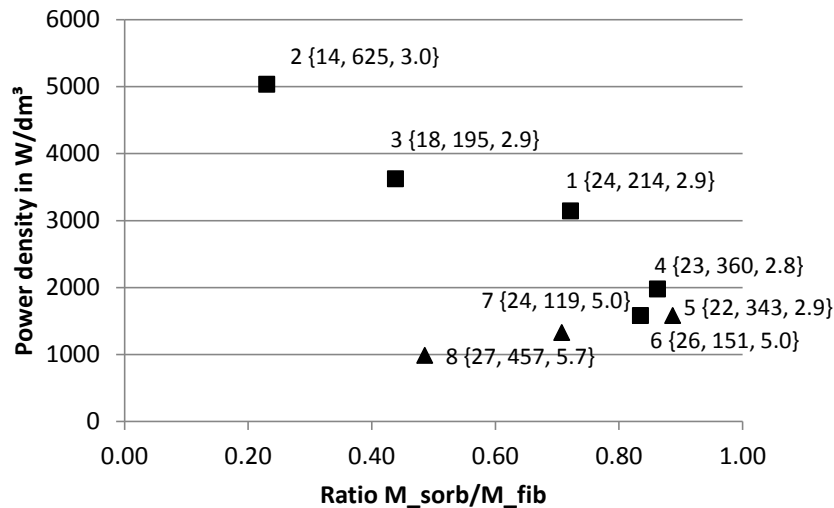


Figure 3 – Mean power density of the measured samples over the ratio of adsorbent mass and fibre mass. The sample properties are shown in brackets $\{d_{cryst}, d_{maP}, d_{cmp}\}$, the rectangle refers to samples with up to 3 mm thickness of the composite, the triangle refers to samples with at least 5 mm thickness of the composite.

In combination with the results for the adsorption dynamics in Figure 2 following conclusions can be drawn:

- Samples 1, 2, and 3 have the highest power densities, for these samples, the power density is decreasing with an increasing adsorbent layer thickness
- The power density of the samples with 3 mm composite thickness (1, 2, 3, 4, 5) decreases nearly linear with the ratio of adsorbent mass to fibre mass. It depends on the optimization criterion (high power density or high COP) which geometry is optimal.
- The relation between power density and rise up time is highly non-linear: The highest power density of sample 2 has the lowest rise up time of only 8.5 s, sample 1 has approx. 60 % of the power density of sample 2 but a half cycle time of approx. 60 s, which is a factor of 8.

CONCLUSION

The fibrous structures presented here offer much degrees of freedom for the design of adsorption heat exchangers and cycles, which means to be able to tailor the adsorption heat exchanger to the needs of the cycle:

- If the hydraulics of the cycle allow very short half cycle times (< 10 s), fibrous structures with a thin adsorbent layer can be used and very high power densities can be achieved
- If the cycle time should be longer due to hydraulic limitations, thicker adsorbent layers can be used, providing still a high power density

The evaluation of the driving temperature differences allows the identification of heat and mass transfer limitations. Although the samples presented here achieve high power densities, there's still some potential for improvement. A good compromise between a high COP (high ratio of sorbent to metal) and a high power density could be a configuration between sample 1 and sample 2: $d_{\text{cmp}}=3\text{mm}$, $d_{\text{cryst}}=15\mu\text{m}$, $d_{\text{fib,pre}}=100\mu\text{m}$, $\psi_{\text{fib,pre}}=0.7$ resulting in a macro pore diameter of $d_{\text{maP}}=200\mu\text{m}$.

REFERENCES

- Andersen, O.; Studnitzky, T.; Kostmann, C.; Stephani, G. (2007): Sintered Metal Fiber Structures from Aluminum Based Fibers-Manufacturing and Properties. In: L. P. Lefebvre, J. Banhart und D. C. Dunand (Hg.): Conf. Proc. MetFoam, S. 509–512.
- Aristov, Yuri (2014): Concept of adsorbent optimal for adsorptive cooling/heating. In: *Applied Thermal Engineering* 72 (2), S. 166–175. DOI: 10.1016/j.applthermaleng.2014.04.077.
- Bauer, J.; Herrmann, R.; Mittelbach, W.; Schwieger, W. (2009): Zeolite/aluminum composite adsorbents for application in adsorption refrigeration. In: *Int. J. Energy Res.* 33 (13), S. 1233–1249. DOI: 10.1002/er.1611.
- Dawoud, Belal (2013): Water vapor adsorption kinetics on small and full scale zeolite coated adsorbents; A comparison. In: *Appl. Therm. Eng.* 50 (2), S. 1645–1651. DOI: 10.1016/j.applthermaleng.2011.07.013.
- Frazzica, Andrea; Földner, Gerrit; Sapienza, Alessio; Freni, Angelo; Schnabel, Lena (2014): Experimental and theoretical analysis of the kinetic performance of an adsorbent coating composition for use in adsorption chillers and heat pumps. In: *Applied Thermal Engineering* 73 (1), S. 1022–1031.
- Földner, Gerrit (2015): Stofftransport und Adsorptionskinetik in porösen Adsorbenskompositen für Wärmetransformationsanwendungen. Dissertation, Freiburg.
- Wittstadt, Ursula; Földner, Gerrit; Andersen, Olaf; Herrmann, Ralph; Schmidt, Ferdinand (2015): A New Adsorbent Composite Material Based on Metal Fiber Technology and Its Application in Adsorption Heat Exchangers. In: *Energies* 8 (8), S. 8431–8446. DOI: 10.3390/en8088431.